

Disrupted Intersubject Variability Architecture in Functional Connectomes in Schizophrenia

Xiaoyi Sun¹⁻³, Jin Liu¹⁻³, Qing Ma¹⁻³, Jia Duan^{4,5}, Xindi Wang¹⁻³, Yuehua Xu¹⁻³, Zhilei Xu¹⁻³, Ke Xu⁶, Fei Wang^{4,6}, Yanqing Tang^{4,5,7}, Yong He¹⁻³, and Mingrui Xia^{*,1-3,7,8}

¹State Key Laboratory of Cognitive Neuroscience and Learning, Beijing Normal University, Beijing 100875, China; ²Beijing Key Laboratory of Brain Imaging and Connectomics, Beijing Normal University, Beijing 100875, China; ³IDG/McGovern Institute for Brain Research, Beijing Normal University, Beijing 100875, China; ⁴Department of Psychiatry, The First Affiliated Hospital of China Medical University, Shenyang 110001, China; ⁵Brain Function Research Section, The First Affiliated Hospital of China Medical University, Shenyang 110001, China; ⁶Department of Radiology, The First Affiliated Hospital of China Medical University, Shenyang 110001, China; ⁷These authors are co-corresponding authors who jointly directed this work.

*To whom correspondence should be addressed; National Key Laboratory of Cognitive Neuroscience and Learning, Beijing Key Laboratory of Brain Imaging and Connectomics, IDG/McGovern Institute for Brain Research, Beijing Normal University, Beijing 100875, China; tel: +86-10-58802036, fax: +86-10-58802036, e-mail: mxia@bnu.edu.cn

Schizophrenia (SCZ) is a highly heterogeneous disorder with remarkable intersubject variability in clinical presentations. Previous neuroimaging studies in SCZ have primarily focused on identifying group-averaged differences in the brain connectome between patients and healthy controls (HCs), largely neglecting the intersubject differences among patients. We acquired whole-brain resting-state functional MRI data from 121 SCZ patients and 183 HCs and examined the intersubject variability of the functional connectome (IVFC) in SCZ patients and HCs. Between-group differences were determined using permutation analysis. Then, we evaluated the relationship between IVFC and clinical variables in SCZ. Finally, we used datasets of patients with bipolar disorder (BD) and major depressive disorder (MDD) to assess the specificity of IVFC alteration in SCZ. The whole-brain IVFC pattern in the SCZ group was generally similar to that in HCs. Compared with the HC group, the SCZ group exhibited higher IVFC in the bilateral sensorimotor, visual, auditory, and subcortical regions. Moreover, altered IVFC was negatively correlated with age of onset, illness duration, and Brief Psychiatric Rating Scale scores and positively correlated with clinical heterogeneity. Although the SCZ shared altered IVFC in the visual cortex with BD and MDD, the alterations of IVFC in the sensorimotor, auditory, and subcortical cortices were specific to SCZ. The alterations of whole-brain IVFC in SCZ have potential implications for the understanding of the high clinical heterogeneity of SCZ and the future individualized clinical diagnosis and treatment of this disease.

Key words: resting-state fMRI/functional connectivity/connectome/individual difference/heterogeneous

Introduction

Schizophrenia (SCZ) is a highly prevalent psychiatric disorder affecting over 20 million people worldwide,¹ and it is accompanied by heterogeneous clinical manifestations, including positive symptoms, negative symptoms, and cognitive deficits.² Growing evidence suggests that SCZ is a brain connectome disorder with dysfunctions spanning from primary to heteromodal areas.³⁻⁵ Nonetheless, findings are often inconsistent across studies, hampering the discovery of validated biomarkers that can guide clinical diagnosis and optimize treatment strategies. A critical reason for this situation is that most prior connectome studies have utilized case-control designs to evaluate the group-averaged differences between patients and healthy controls (HCs). The intersubject differences in the connectome architecture among patients with SCZ have been largely understudied.

The resting-state functional magnetic resonance imaging (R-fMRI) technique provides an unprecedented opportunity to noninvasively investigate the intrinsic connectome architecture of the brain in vivo.^{6,7} In particular, recent progress in R-fMRI has moved towards characterizing the intersubject variability of the functional connectome (IVFC). The IVFC of each network node was estimated by subtracting the averaged intersubject similarity of the nodal functional connectivity profiles from one. In the healthy population, the whole-brain IVFC pattern exhibits a nonuniform distribution, with higher variability in the heteromodal cortices and lower variability in the primary cortices.⁸⁻¹¹ Such a pattern is compatible with our understanding of

individual differences in cognitive functions. In SCZ, although a few studies have found high heterogeneity of functional connections in focal regions (eg, the dorsolateral prefrontal cortex)¹² and functional components (eg, sensorimotor, visual, and auditory components),^{13,14} the whole-brain IVFC pattern remains largely unclear. More importantly, it is of great interest whether the IVFC pattern is altered in SCZ patients relative to healthy subjects, and if so, whether these alterations are specific to SCZ or are general to other psychiatric disorders such as bipolar disorder (BD) and major depressive disorder (MDD).

To address these issues, in this study, we collected R-fMRI data from 121 SCZ patients and 183 matched HCs. Using a voxelwise whole-brain connectivity analysis, we identified alterations in IVFC in SCZ, and we further examined the relationship of these alterations with the clinical variables in the patients. To determine the specificity of the connectivity alterations, we also analyzed the IVFC in BD and MDD.

Methods

Participants

Three R-fMRI datasets were included in this study. The principal dataset (dataset 1) included 139 patients with SCZ and 189 HCs. The validation datasets included 108 patients with BD (dataset 2) and 114 patients with MDD (dataset 3). All patients were enrolled from the inpatient and outpatient services at Shenyang Mental Health Center and the Department of Psychiatry, First Affiliated Hospital of China Medical University, Shenyang, China. HCs were recruited via local advertisements. The diagnosis of patients was performed together by 2 experienced psychiatrists. Patients aged 18 years and older were diagnosed using the criteria from the Structured Clinical Interview for Diagnostic and Statistical Manual of Mental Disorders Fourth Edition, whereas patients under 18 years old were diagnosed using the criteria supplied by the semistructured diagnostic interview for the Schedule for Affective Disorders and Schizophrenia for School-Age Children-Present and Lifetime Version. All patients met the diagnostic criteria for SCZ, BD, or MDD and had no other Axis I disorder. The HCs did not have a current or lifetime history of an Axis I disorder or a history of psychotic, mood, or other Axis I disorders in first-degree relatives. The exclusion criteria for all participants included MRI contraindications, a history of drug or alcohol abuse, concomitant major medical disorder, a history of head trauma with consciousness disturbances or any neurological disorders, and suboptimal imaging data quality. Finally, 121 patients with SCZ, 183 HCs, 100 patients with BD, and 108 patients with MDD were included. The clinical symptoms and cognitive measures were assessed using the Brief Psychiatric Rating Scale (BPRS), Hamilton Depression Rating Scale (HAM-D), Hamilton Anxiety Rating Scale (HAMA), Young Mania

Rating Scale (YMRS), and Wisconsin Card Sorting Test (WCST). Disease duration, medication status, episode status, and onset age were collected for each patient. This study was approved by the Institutional Review Board of China Medical University. Written informed consent was obtained from all participants. The datasets have previously been used in the graph-theory analyses of functional brain networks and brain modules.^{15,16}

Data Acquisition

R-fMRI data were collected on a GE Signa HD 3.0T scanner (General Electric) with a standard 8-channel head coil at the First Affiliated Hospital of China Medical University, Shenyang, China ([supplementary material](#)). The scan lasted for 6 minutes and 40 seconds, resulting in 200 volumes. The participants were instructed to rest and relax with their eyes closed, but to keep from falling asleep during scanning.

Data Preprocessing

R-fMRI data were preprocessed using SPM12 and DPARSF,¹⁷ including removal of the first 10 volumes, correction for slice-timing and head motion, spatial normalization with 3 mm isotropic voxels, spatial smoothing, linear detrending, regression of nuisance signals (Friston-24 motion parameters, white matter, and cerebrospinal fluid signals) and temporal band-filtering (0.01–0.1 Hz). The global signal was not regressed out in our main analysis because of its neurobiological significance in SCZ.¹⁸ Volume censoring movement correction¹⁹ was finally performed that volumes with a framewise displacement exceeding 0.5 mm and their adjacent volumes were replaced with the linear interpolated data.

Whole-Brain IVFC Pattern and Group Differences

We assessed the IVFC patterns in SCZ and HCs using the procedure proposed by Mueller and colleagues.⁸ For each participant, we first calculated the functional connectivity profiles by performing a voxelwise whole-brain connectivity analysis. Then, for each voxel, the intersubject similarity was assessed by computing the Pearson correlation of functional connectivity profiles between any 2 participants and the IVFC was estimated by subtracting the averaged intersubject similarity from one ([figure 1A](#) and [supplementary material](#)). Thus, the whole-brain IVFC map can be obtained for each group. To test whether the IVFC patterns were significantly different between SCZ and HCs, we compared the global measures of the IVFC maps (the mean and standard deviation) and identified SCZ-related alteration at voxel level by performing a non-parametric permutation test with significant level of $P < .01$ for voxel and $P < .05$ for cluster size (10 000 times, [supplementary material](#)).

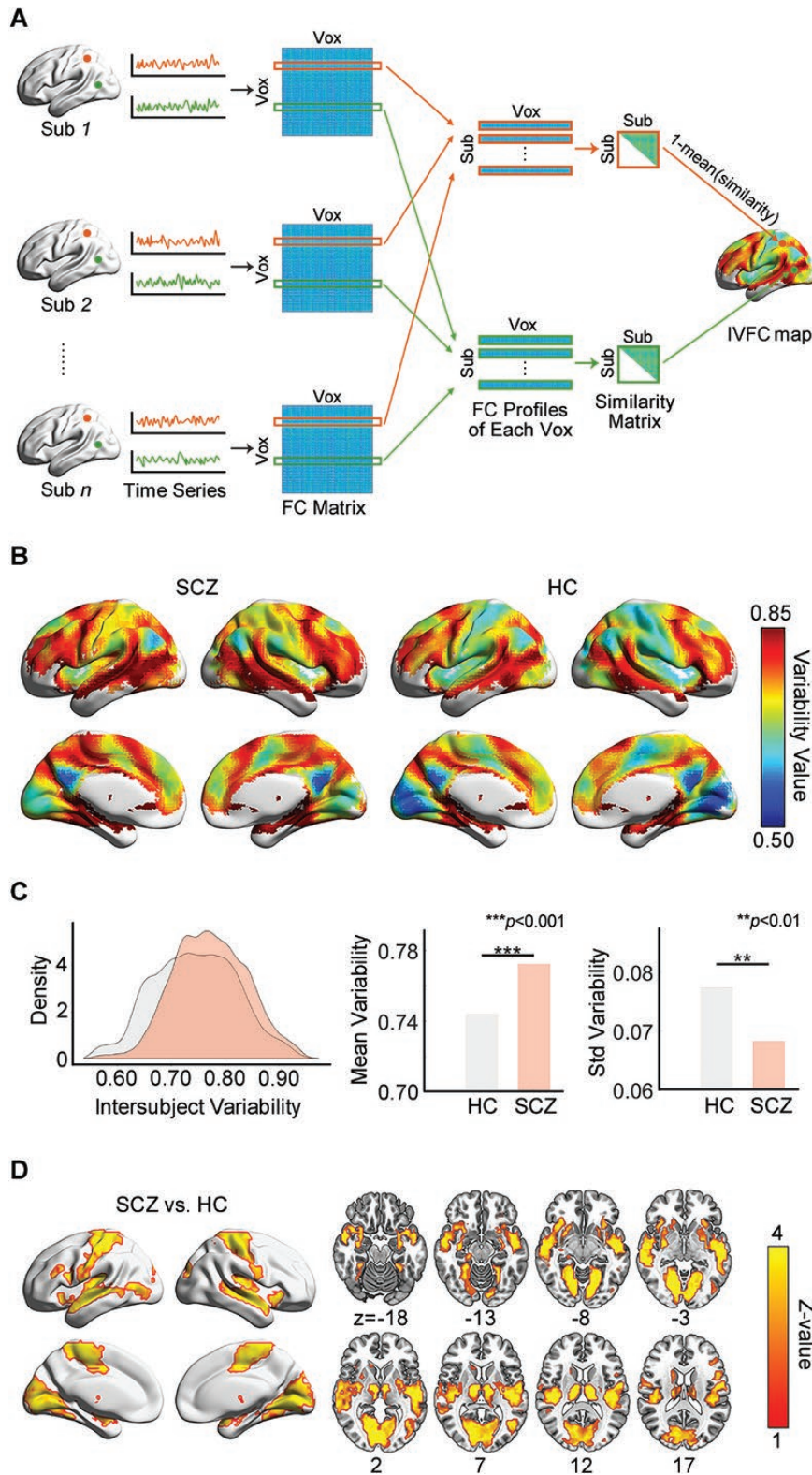


Fig. 1. Disrupted intersubject variability architecture of the brain functional connectome in SCZ. (A) Flow chart for the calculation of intersubject variability. (B) Intersubject variability pattern in the SCZ and HC groups. (C) Comparison of the density distribution, mean value and standard deviation of whole-brain intersubject variability between the SCZ and HC groups. (D) SCZ-related regional alterations in intersubject variability. SCZ: schizophrenia; HC: healthy control; Sub: subject; Vox: voxel; FC: functional connectivity; IVFC: intersubject variability of the functional connectome.

Edgewise Contribution to SCZ-Related Alterations in IVFC

To explore the critical connections that predominately contributed to the IVFC alterations in SCZ, we performed an edgewise variability quantification analysis. We first identified local peaks in clusters exhibiting significant between-group IVFC differences. For each peak, we extracted its functional profiles and estimated the weight of each connection on intersubject similarity by decomposing the standard Pearson's correlation formula in the SCZ and HC groups. Finally, a between-group difference contribution (DC) of each connection was defined as the difference between the reversed intersubject similarity weight (figure 2A and supplementary material). Thus, a DC map representing the contribution to the IVFC differences between SCZ and HC was obtained for each peak.

To further classify the critical connections, we performed agglomerative hierarchical clustering analysis on these DC maps (supplementary material). The optimal number of categories was determined as the minimum value of the maximum mean silhouette value.²⁰ The representative maps were obtained by averaging the contribution maps of all peaks within each category. We demonstrated the 90th percentile of connections with

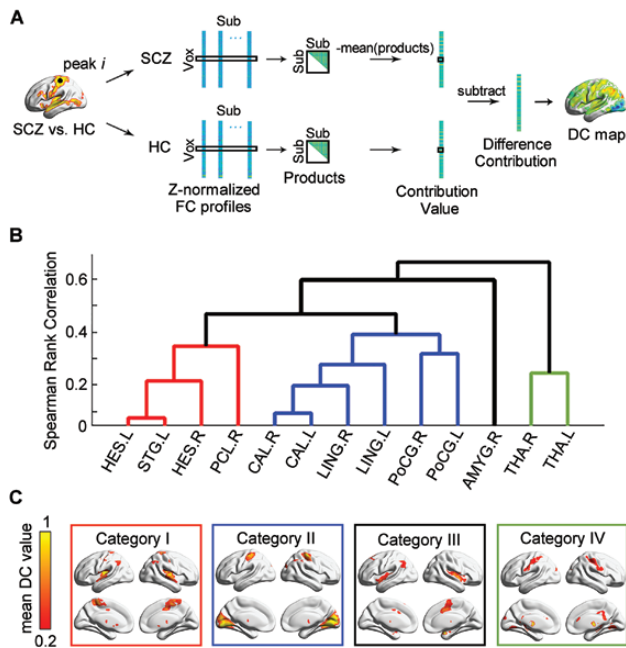


Fig. 2. Edgewise contributions to intersubject functional variability. (A) Flow chart for the calculation of difference contribution. (B) Hierarchical clustering results of difference contribution maps. (C) Mean difference contribution maps of 4 typical categories. SCZ: schizophrenia; HC: healthy control; Sub: subject; Vox: voxel; FC: functional connectivity; DC: difference contribution; HES: Heschl gyrus; STG: superior temporal gyrus; PCL: paracentral lobule; CAL: calcarine fissure and surrounding cortex; LING: lingual gyrus; PoCG: postcentral gyrus; AMYG: amygdala; THA: thalamus.

the top contributions for each category. A cluster-level permutation test with a significance level of $P < .05$ was performed to control the false positive rate (2 other thresholds, the 95th and 85th percentiles, were also calculated; see [supplementary material](#)).

Relationship Between IVFC Patterns and Clinical Variables in SCZ

To investigate the relationship between IVFC and clinical variables in SCZ group, we applied a multiple regression model and bootstrap sampling. In each sampling, 50 subjects (sizes 30 and 70 were also used for validation) were randomly selected, and their IVFC for each local peak and the mean clinical variables, including age of onset, duration, and BPRS, were calculated. This sampling was repeated 10 000 times, and the regression model was built with sampled IVFC as the dependent variables, mean clinical variables as independent variables, and age and gender as covariates. The significance of each dependent variable in the model was determined using permutation test (supplementary material). Furthermore, to characterize the linkage between the heterogeneity of clinical symptoms and functional connectivity, we also calculated the intersubject variability within the 18-item BPRS score and assessed its relationship to IVFC by performing a similar bootstrap sampling analysis (supplementary material). To correct for multiple comparisons, the Bonferroni correction at $P < .05$ across all peaks and clinical variables was applied.

Disorder Specificity of IVFC in SCZ

Common alterations in functional connectivity have been reported in patients with SCZ and other psychiatric disorders such as MDD and BD.^{16,21–28} To assess the specificity of the IVFC alterations in SCZ, we computed the IVFC maps in the MDD and BD groups, followed by permutation tests, as described above.

Validation Analysis

To assess the reliability of our results, we examined the influences of the clinical and demographic variables (ie, participants' age, medication status, and episode status of the disorder) and estimated the effect of image preprocessing (ie, global signal removal and head motion). To reduce the confounding factor of intrasubject variance in functional connectivity profiles, we also re-estimated IVFC patterns for each group by splitting the participants' time points into 2 halves (supplementary material).

Results

Demographics and Clinical Characteristics

There were no significant differences in age, gender, handedness, or smoking history among the 4 groups.

Age onset also did not differ among the 3 patient groups. However, significant differences were observed in illness duration, first-episode status, medication status, HAMD, HAMA, YMRS, and BPRS scores among 3 patient groups ($P < .001$). A direct comparison between HC and SCZ groups revealed no significant differences in age, gender, handedness, or smoking history. However, patients with SCZ had significantly higher scores in HAMD, HAMA, YMRS, and BPRS than the HCs ($P < .001$, [table 1](#)).

Abnormal Whole-Brain IVFC Pattern in SCZ

The whole-brain IVFC pattern in the SCZ group was remarkably similar to that in the HCs ($r = .93$, $P < .0001$), with higher IVFC in the heteromodal association cortex, including the lateral prefrontal, parietal, and temporal cortices, and lower IVFC in the primary sensorimotor and visual areas ([figure 1B](#)). The SCZ group showed a significantly higher global mean variability ($P < .001$) and a lower standard deviation of variability ($P = .003$).

Table 1. Demographics and Clinical Characteristics of the Participants

	Datasets 1		Datasets 2		Datasets 3	
	Healthy Control ($n = 183$)	Schizophrenia ($n = 121$)	Bipolar Disorder ($n = 100$)	Major Depressive Disorder ($n = 108$)	Statistical Test F/χ^2 (P)	HC vs SCZ Statistical Test T/χ^2 (P)
Demographic characteristics						
Age at scanning, years	26.62 (8.00)	24.74 (9.03)	25.81 (8.31)	25.62 (8.43)	1.26 (0.288)	1.85 (0.065)
Gender (male/female)	73/110	54/67	48/52	35/73	6.07 (0.108)	0.67 (0.412)
Handedness (Right/Left/Bilateral) ^a	172/0/8	100/2/10	95/1/2	96/2/3	10.23 (0.115)	5.76 (0.056)
Smoking history (smoking/no smoking) ^a	29/128	12/76	21/62	22/67	5.12 (0.163)	0.95 (0.331)
Clinical characteristics						
Age at illness onset	-	22.82 (8.89)	21.72 (7.24)	23.57 (8.20)	1.15 (0.318)	-
Illness duration, months	-	21.87 (36.15)	41.48 (56.18)	20.58 (31.00)	7.23 (0.001)	-
First episode, yes ^a	-	86 (74%)	52 (57%)	85 (88%)	34.78 (<0.001)	-
Medication, yes ^a	-	71 (59%)	65 (65%)	43 (40%)	172.36 (<0.001)	-
Antidepressants, yes ^a	-	4 (4%)	28 (29%)	35 (36%)	32.68 (<0.001)	-
Antipsychotics, yes ^a	-	59 (61%)	35 (36%)	1 (1%)	78.54 (<0.001)	-
Mood stabilizer, yes ^a	-	4 (4%)	52 (53%)	0	116.53 (<0.001)	-
HAMD-17	($n = 165$) 1.17 (1.67)	($n = 86$) 8.12 (6.96)	($n = 99$) 11.77 (9.48)	($n = 107$) 21.16 (8.77)	186.93 (<0.001)	-9.12 (<0.001)
HAMA	($n = 164$) 0.77 (1.76)	($n = 69$) 6.80 (7.26)	($n = 96$) 8.52 (8.80)	($n = 93$) 16.32 (9.49)	103.51 (<0.001)	-6.80 (<0.001)
YMRS	($n = 158$) 0.15 (0.57)	($n = 60$) 2.20 (4.50)	($n = 95$) 8.07 (10.05)	($n = 89$) 1.47 (2.87)	45.29 (<0.001)	-3.51 (0.001)
BPRS	($n = 96$) 18.30 (0.68)	($n = 116$) 35.59 (14.32)	($n = 60$) 25.83 (8.38)	($n = 46$) 25.41 (6.08)	57.01 (<0.001)	-12.99 (<0.001)
Cognitive function						
WCST	($n = 110$)	($n = 58$)	($n = 58$)	($n = 66$)	-	-
Correct responses	29.13 (12.66)	18.14 (11.78)	23.47 (12.31)	23.27 (11.91)	10.80 (<0.001)	5.48 (<0.001)
Categories completed	3.81 (2.28)	1.57 (1.80)	2.69 (2.07)	2.83 (2.04)	14.93 (<0.001)	6.50 (<0.001)
Total errors	19.06 (12.74)	29.86 (11.78)	24.02 (12.41)	24.80 (11.91)	10.24 (<0.001)	-5.36 (<0.001)
Perseverative errors	7.36 (7.92)	13.36 (12.52)	10.03 (10.28)	10.83 (9.60)	5.05 (0.002)	-3.32 (0.001)
Non-perseverative errors	11.56 (7.08)	16.50 (8.80)	14.36 (7.72)	13.97 (6.53)	5.93 (0.001)	-3.70 (<0.001)
Head motion parameters						
Max translation, mm	0.56 (0.39)	0.67 (0.49)	0.66 (0.47)	0.68 (0.58)	1.89 (0.130)	-1.81 (0.072)
Max rotation, degree	0.55 (0.42)	0.64 (0.51)	0.61 (0.44)	0.66 (0.58)	1.64 (0.180)	-1.67 (0.096)
Mean FD, mm	0.11 (0.05)	0.12 (0.08)	0.12 (0.06)	0.11 (0.06)	2.12 (0.096)	-1.86 (0.064)
FD _ Percentage	0.01 (0.03)	0.02 (0.05)	0.02 (0.04)	0.02 (0.04)	2.25 (0.081)	-1.98 (0.049)

Note: Data are presented as either n (%) or means (SDs). HAMD-17, Hamilton Depression Scale; HAMA, Hamilton Anxiety Scale; YMRS, Young Mania Rating Scale; BPRS, Brief Psychiatric Rating Scale; WCST, Wisconsin Card Sorting Test; FD, framewise displacement.

^aInformation was missing for some participants.

than the HC group (figure 1C). This result suggests that the SCZ group tended to have higher across-subject heterogeneity and simultaneously reduced across-regional diversity in the whole-brain functional connectome than the HC group. Regionally, the SCZ group had a significantly higher IVFC in the bilateral sensorimotor, visual, auditory, and subcortical regions ($P < .05$, 10 000 permutations corrected, figure 1D and supplementary table S1).

Edgewise Contributions to SCZ-Related Alterations in IVFC

We identified the critical connections that contributed to alterations of IVFC in SCZ (supplementary figure S1), which were mainly classified into 4 categories (figure 2 and supplementary figure S2): (1) connections of the bilateral Heschl gyrus (HES), the left superior temporal gyrus (STG), and the right paracentral lobule (PCL) ($P < .05$, 10 000 permutations corrected, figure 2 and supplementary table S2), which are mainly related to auditory perception and language processing; (2) connections of the bilateral calcarine (CAL), the lingual gyrus (LING), and the postcentral gyrus (PoCG) (figure 2 and supplementary table S3), which are primarily involved in sensorimotor and visual processing; (3) connections of the right amygdala (AMYG) (figure 2 and supplementary table S4), which is dominantly related to emotional and social cognition regulation; (4) connections of the bilateral thalamus (THA) (figure 2 and supplementary table S5), which is involved in sensory information integration and mental coordination. The validation test showed that the number of connections extracted did not change the significant regions with edgewise contributions to the IVFC for each category (supplementary figure S3).

Clinical Relevance of Intersubject Variability

The IVFC was negatively correlated with the age of onset ($t = -10.52 \pm 5.21$, $P < .001$ Bonferroni-corrected) in the bilateral CAL, LING, and PoCG; right HES, PCL, and AMYG; and left THA and STG, with the disease duration ($t = -9.58 \pm 3.64$, $P < .001$ Bonferroni-corrected) in bilateral CAL and LING; right HES, PCL, and AMYG; and left STG and PoCG, and with the BPRS ($t = -13.85 \pm 6.00$, $P < .001$ Bonferroni-corrected) in bilateral CAL, THA, and LING; right AMYG; and left PoCG and STG (figure 3A and supplementary table S6). Further analyses showed that IVFC was positively correlated with the within-BPRS heterogeneity ($t = 12.52 \pm 3.91$, $P < .001$ Bonferroni-corrected) in the bilateral HES, CAL and LING; right AMYG and PCL; and left PoCG and STG (figure 3A and supplementary table S7). The sample size of bootstrapping did not change the relevance (supplementary tables S8–S10). Moreover, when dividing patients into subgroups according to their clinical status (ie, medication and episode), we found that

the non-medicated and first-episode subgroups had an additionally broader disrupted variability than the medicated (figure 3B) and recurrent subgroups (figure 3C), respectively.

Disorder Specificity of IVFC in SCZ

Both the BD and MDD groups exhibited similar spatial patterns to the HC group (BD: $r = .96$, MDD: $r = .97$, both $P < .0001$) (figure 4). Voxelwise comparison showed that the medial occipital cortex exhibited significantly higher IVFC in the BD and MDD groups than in the HC group, and this region was also the altered region shared with the SCZ group ($P < .05$ permutation-corrected) (figure 4, supplementary tables S11 and S12). However, there was a broader regional higher variability in SCZ, including the bilateral sensorimotor, auditory, and subcortical regions, indicating the relative specificity of SCZ-related alterations of IVFC (figure 4).

Validation Results

Generally, the altered IVFC pattern in SCZ remained largely unchanged in the validation, including the participants' age (supplementary figure S4), global signal removal (supplementary figure S5), intrasubject variance (supplementary figure S6), and head motion (supplementary figures S7, S8, and table S13). However, the global signal and intrasubject variance regression led to SCZ-related higher IVFC in the lateral frontal cortex and anterior cingulate gyrus (supplementary figures S5 and S6).

Discussion

In this study, we systematically investigated the whole-brain voxelwise IVFC pattern in patients with SCZ. Specifically, we found that the spatial distribution of the IVFC pattern was similar between the SCZ and HC groups. However, the SCZ group exhibited significantly higher IVFC than the HC group in the sensorimotor, visual, auditory, and subcortical cortex, and the altered IVFC was significantly correlated with clinical scores. The alteration of IVFC was relatively specific to SCZ, while the visual cortex was a shared altered region among SCZ, BD, and MDD, and the sensorimotor, auditory, and subcortical cortices were only altered in SCZ. Together, these findings provide mechanistic insights into the observed inconsistent dysconnectivity results in previous studies and inspire imaging-derived candidate phenotypes for the guidance of individualized clinical diagnosis and treatment evaluations.

Disrupted Whole-Brain IVFC in SCZ

The higher whole-brain mean variability and lower standard deviation of variability indicated a higher global individual variability across patients and lower

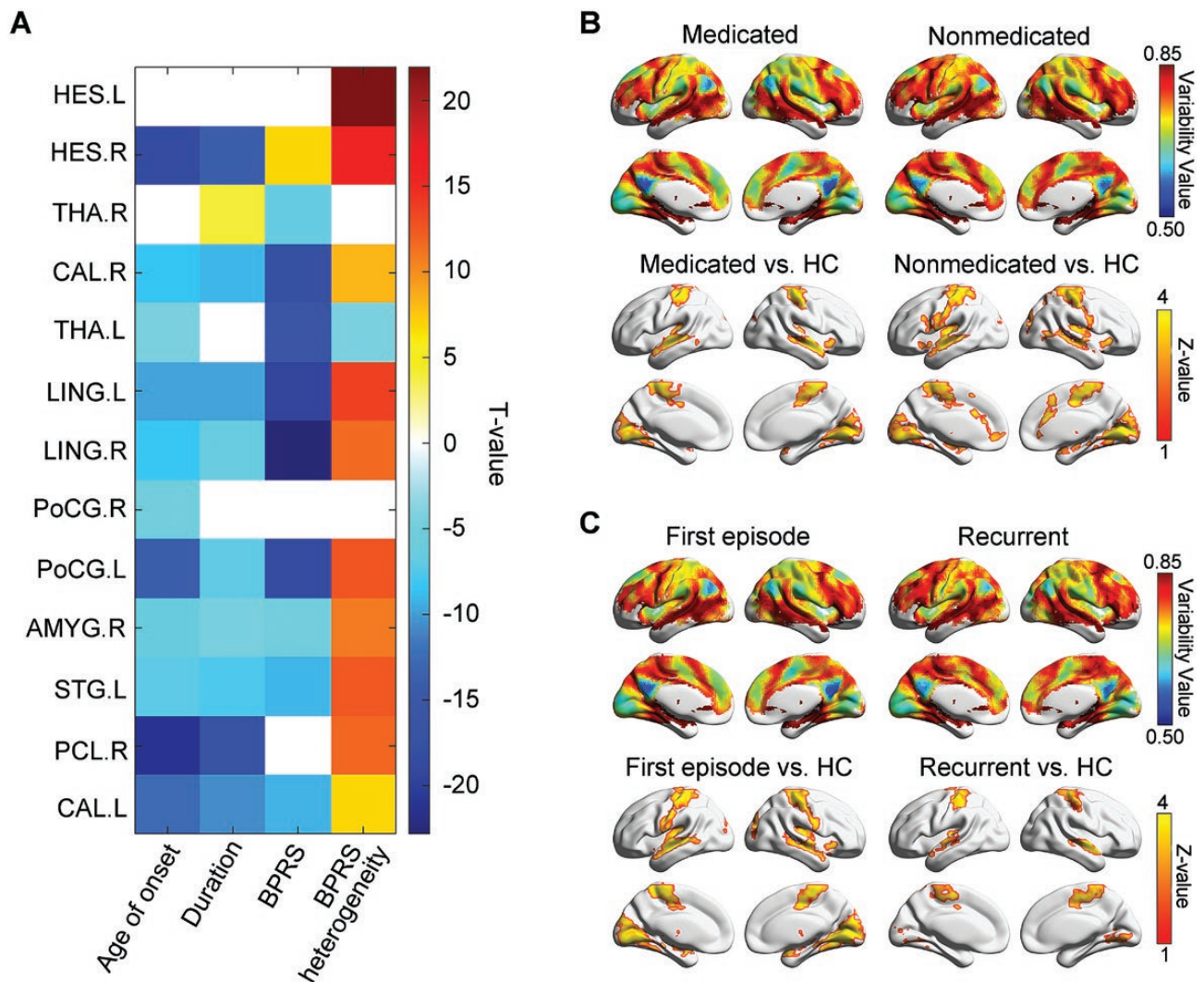


Fig. 3. The clinical relevance of intersubject variability. (A) Relationship between intersubject variability and clinical variables. A non-white grid indicates a significant correlation with a Bonferroni-corrected $P < .05$. (B) Effects of the medication status of SCZ patients on the calculation of intersubject functional variability. (C) Effects of the episode status of SCZ patients on the calculation of intersubject functional variability. HC, healthy control; HES: Heschl gyrus; THA: thalamus; CAL: calcarine fissure and surrounding cortex; LING: lingual gyrus; PoCG: postcentral gyrus; AMYG: amygdala; STG: superior temporal gyrus; PCL: paracentral lobule; BPRS: Brief Psychiatric Rating Scale.

heterogeneity across brain regions in SCZ. These results are largely comparable with the previous findings of randomized functional connectivity¹⁶ and dedifferentiation across whole functional systems in SCZ.¹⁵ Our additional statistical analysis showed that IVFC was negatively correlated to the clustering coefficient, characteristic shortest path length, and modularity in SCZ (supplementary table S14). These findings indicate that the functional connectivity became more heterogeneity among patients as their brain connectome became more randomized. Regionally, higher IVFC of the sensorimotor, visual, auditory, and subcortical cortex were found in SCZ. Altered functional connectivity of these regions has generally been reported and is related to bottom-up processing and integration, emotional dysfunction, and social cognition impairments in SCZ.^{4,5,16,29-35} The greater

IVFC of these regions might imply that the decoding and integrating processing of primary sensory input are different among patients before higher-level processes, which could partially explain the high heterogeneity of clinical symptoms and the diverse dysconnectivity observed across studies in SCZ.^{5,36-39} Moreover, physiological changes in these regions were also found in previous studies.⁴⁰⁻⁴⁴ Participants with SCZ or at high risk for SCZ showed significant elevations in glutamate, glutamine or Glx (glutamate + glutamine) in the basal ganglia, thalamus, and medial temporal lobe. These abnormal metabolites were related to the illness phase⁴² and indicated different potential physiological factors across SCZ patients. Higher heterogeneity of abnormal structural measures were also found in SCZ.⁴⁵⁻⁴⁸ Our findings of higher IVFC in sensorimotor, visual, auditory, and subcortical

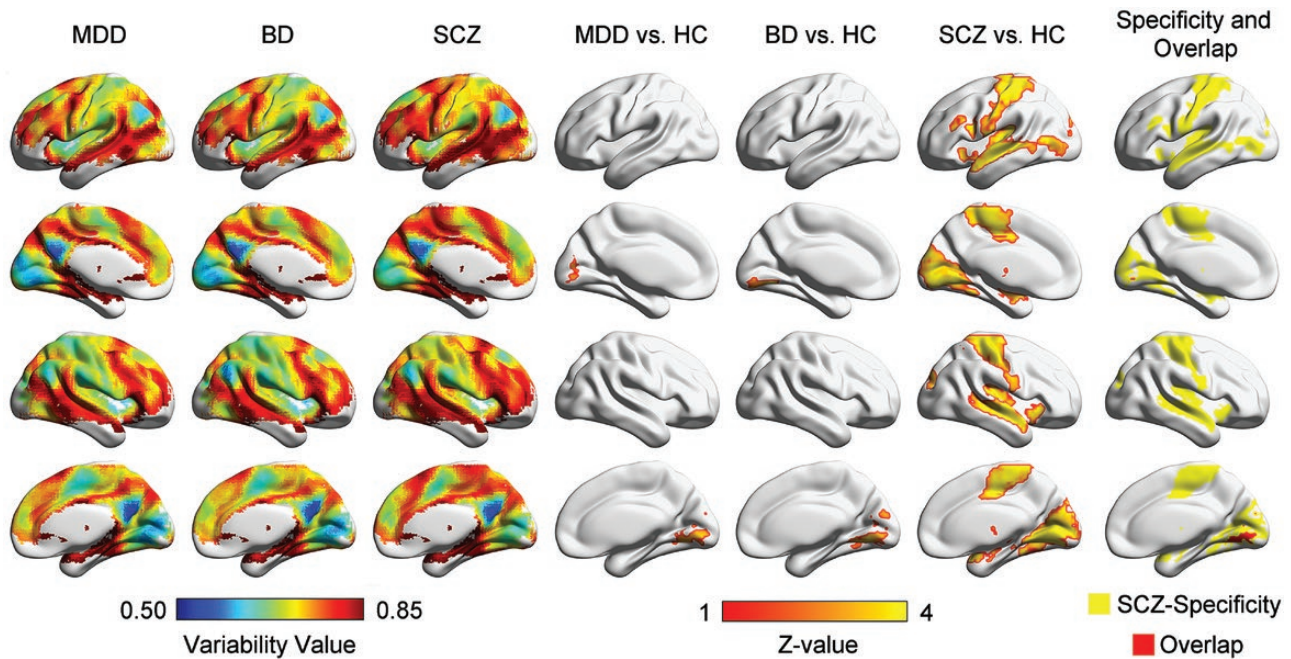


Fig. 4. Disorder specificity of intersubject functional variability in SCZ. Columns 1 to 3 are the spatial patterns of the intersubject variability in the MDD, BD, and SCZ groups. Columns 4 to 6 are the MDD-, BD-, and SCZ-related alterations in intersubject functional variability. Column 7 is the comparison of the altered intersubject variability of MDD, BD, and SCZ. The yellow patches indicate the SCZ-specificity alterations, and the red patches indicate the overlapped alterations of 3 disorders. SCZ: schizophrenia; BD: bipolar disorder; MDD: major depressive disorder.

regions are largely comparable with the structural observations. The inconsistency between the 2 modalities occurred mainly in the frontal cortex. It is consistent with finding that structure-function coupling is weaker in the transmodal than unimodal regions.⁴⁹ However, the correspondence between functional and structural variability in SCZ remains largely unknown, and further research may provide a structural basis for the IVFC alteration.

Critical Contribution Connections to SCZ-Related IVFC Alterations

We found that the connections with the top contributions to IVFC in SCZ involved several different pathways. Specifically, the temporoparietal junction (TPJ) is one of the most involved regions connecting to the auditory, sensorimotor, and visual cortices, as well as the AMYG. Previous studies have shown that the connections between the TPJ and these areas are related to perceptual abnormalities and external/inner voices differentiate inability in SCZ.⁵⁰⁻⁵⁵ The increased IVFC of TPJ might thus point to different forms of self-consciousness delusions, auditory-verbal hallucinations, and social responses among patients. Moreover, our findings provide an interpretation of the mixed results for dysconnectivity in the TPJ with both hyper- and hypo-connectivity reported in previous studies.⁵¹ THA connections, involving primary, limbic, and subcortical areas, also contribute largely to the high variability in SCZ. The cortico-striatal-thalamic-AMYG

pathway is a classical reward/punishment model related to motivation and goal-directed behavior^{31,56,57} and is involved in emotional memory and effective perception of fear signals.⁵⁸⁻⁶⁰ Impaired functional connectivity of this pathway has been reported in the SCZ, which is most pronounced in patients with negative symptoms.^{31,61} This pathway belongs to the substantia nigra-based subcortical-cortical motor circuit⁶²⁻⁶⁴ and closely related to the disrupted serotonin (5-HT), dopamine, and glutamate activity.^{63,65-68} Considering the different findings for dysconnectivity and the correlation between dysconnectivity and clinical scores among studies,^{25,60,69-72} our results suggest that the intersubject difference in functional connectivity may contribute to the different negative symptoms and task responses among patients.

Relationship Between IVFC and Clinical Variables

We found that the IVFC is negatively correlated with age onset. This is consistent with previous finding that childhood-/early-onset SCZ patients exhibit severer functional connectivity abnormalities and clinical manifestations than adult-onset patients.⁷³⁻⁷⁵ A potential explanation may be due to the high plasticity of brain development in childhood.⁷⁶ Evidence has shown that a longer disease duration and higher clinical severity are positively correlated with the functional connectivity abnormalities in SCZ.^{71,72,77-80} The negative correlation between IVFC and these 2 clinical variables observed herein indicates that

the altered brain architecture of patients becomes more convergent as the duration and clinical severity increases. Furthermore, the positive correlation between IVFC and the intersubject variability of 18-items BPRS scores highlights the correspondence between clinical heterogeneity and functional connection heterogeneity, indicating the potential implications of our findings for understanding the high clinical heterogeneity of SCZ. Future analysis based on clinical information in single symptom dimensions, such as the Positive and Negative Syndrome Scale, may reflect more factors related to IVFC across SCZ patients.

The difference between IVFC of medicated and non-medicated subgroups is consistent with previous evidence that non-medicated patients exhibit broader abnormalities in functional connectivity.^{78,81} Studies also showed that functional connectivity of the medial prefrontal cortex, anterior cingulate, and THA can be largely improved after antipsychotic medications.^{82–85} Altogether, these results validate that non-medicated patients exhibit more severity and differences among patients. Besides, our results of the first-episode subgroup exhibited more alteration than the recurrent subgroup (figure 3C), potentially because most of the patients in the first-episode subgroup were non-medicated.

Disorder Specificity of IVFC in SCZ

MDD, BD, and SCZ are 3 complex brain dysconnectivity disorders characterized by various clinical symptoms.^{86–88} Because of the overlapping clinical symptoms across these 3 disorders, clinical differential diagnosis has been a major challenge.⁸⁹ Recently, increasing neuroimaging studies have focused on the transdiagnostic common and specific alterations in functional brain networks among psychiatric disorders.^{15,16,90} A brain structure study showed that the distribution of reduced gray matter among SCZ patients had wide intersubject variability involving frontal, temporal, and cerebellar regions, while that among BD patients was only found in cerebellar regions.⁴⁸ Comparable to the previous study, our results provide novel evidence of SCZ-specific broader alterations in IVFC compared with BD and MDD from a functional connectome perspective. The specific IVFC alterations in sensorimotor, auditory, and subcortical areas might indicate a more complex heterogeneous pathology in SCZ and provide insight into the search for disease-specific biomarkers.

Limitations and Future Directions

Several issues of the current study need to be further addressed. First, all participants were instructed to keep awake during scanning. Although all participants reported being awake after scanning, we cannot ensure the validity. Further studies using equipment that monitors

eye movements or records physiological signals during the R-fMRI scan can better address this issue. Second, studies have shown that a resting-state scan longer than 6 minutes can increase the reliability of measuring individual differences in terms of strength of connectivity.^{91,92} Further analysis based on fMRI data longer than 6 minutes may have more stable results in the assessment of intersubject variability. Third, several different methods have been used to study heterogeneity in functional connectivity in SCZ, including regional seed-based connectivity,¹² independent vector analysis,¹³ and group independent component analysis.¹⁴ Interestingly, all these methods showed higher individual variability in SCZ, although the measurements and observation levels differed. Besides demonstrating the whole-brain IVFC pattern at a finer voxel-level, the method of the current study also can identify critical pathways that contribute to the IVFC in a data-driven manner. Nonetheless, novel methods and models are required to delineate inter-subject variability in SCZ from multiple perspectives. Fourth, the high heterogeneity of the brain functional connectome among SCZ patients might suggest the presence of different pathologies in SCZ. A recent study has shown potential genetic associations to brain functional component variability,¹⁴ clarification of the neurophysiological subtypes in SCZ combining the individual functional connectome and biological data (eg, gene expression) could highly contribute to our understanding of SCZ pathology. Finally, our results also provide an explanation for the currently unsatisfactory imaging-based individual diagnosis, treatment prediction, and stimulation target optimization in SCZ. Developing biomarkers based on an individualized connectome analysis framework is becoming a valuable direction in developing precision medication for the treatment of SCZ.

Supplementary Material

Supplementary material is available at *Schizophrenia Bulletin* online.

Funding

National Natural Science Foundation of China (81671767, 82071998 to M.X. and 81620108016 to Y.H.), Beijing Nova Program (Z191100001119023 to M.X.), Changjiang Scholar Professorship Award (T2015027 to Y.H.), Beijing Municipal Science & Technology Commission (Z161100004916027 to Y.H.), Fundamental Research Funds for the Central Universities (2020NTST29 to M.X.).

Acknowledgments

The authors have declared that there are no conflicts of interest in relation to the subject of this study.

References

1. James SL, Abate D, Abate KH, et al. Global, regional, and national incidence, prevalence, and years lived with disability for 354 diseases and injuries for 195 countries and territories, 1990–2017: a systematic analysis for the Global Burden of Disease Study 2017. *The Lancet* 2018;392(10159):1789–1858.
2. Owen MJ, Sawa A, Mortensen PB. Schizophrenia. *Lancet*. 2016;388(10039):86–97.
3. Fornito A, Zalesky A, Pantelis C, Bullmore ET. Schizophrenia, neuroimaging and connectomics. *Neuroimage*. 2012;62(4):2296–2314.
4. Skåtun KC, Kaufmann T, Doan NT, et al.; KaSP. Consistent functional connectivity alterations in schizophrenia spectrum disorder: a multisite study. *Schizophr Bull*. 2017;43(4):914–924.
5. Dong D, Wang Y, Chang X, Luo C, Yao D. Dysfunction of large-scale brain networks in schizophrenia: a meta-analysis of resting-state functional connectivity. *Schizophr Bull*. 2018;44(1):168–181.
6. Biswal B, Yetkin FZ, Haughton VM, Hyde JS. Functional connectivity in the motor cortex of resting human brain using echo-planar MRI. *Magn Reson Med*. 1995;34(4):537–541.
7. Fox MD, Greicius M. Clinical applications of resting state functional connectivity. *Front Syst Neurosci*. 2010;4:19.
8. Mueller S, Wang D, Fox MD, et al. Individual variability in functional connectivity architecture of the human brain. *Neuron*. 2013;77(3):586–595.
9. Gao W, Elton A, Zhu H, et al. Intersubject variability of and genetic effects on the brain's functional connectivity during infancy. *J Neurosci*. 2014;34(34):11288–11296.
10. Xu Y, Cao M, Liao X, et al. Development and emergence of individual variability in the functional connectivity architecture of the preterm human brain. *Cereb Cortex*. 2019;29(10):4208–4222.
11. Liao X, Cao M, Xia M, He Y. Individual differences and time-varying features of modular brain architecture. *Neuroimage*. 2017;152:94–107.
12. Cole MW, Anticevic A, Repovs G, Barch D. Variable global dysconnectivity and individual differences in schizophrenia. *Biol Psychiatry*. 2011;70(1):43–50.
13. Gopal S, Miller RL, Michael A, et al. Spatial variance in resting fmri networks of schizophrenia patients: an independent vector analysis. *Schizophr Bull*. 2016;42(1):152–160.
14. Chen J, Rashid B, Yu Q, et al. Variability in resting state network and functional network connectivity associated with schizophrenia genetic risk: a pilot study. *Front Neurosci*. 2018;12:114.
15. Ma Q, Tang Y, Wang F, et al. Transdiagnostic dysfunctions in brain modules across patients with schizophrenia, bipolar disorder, and major depressive disorder: a connectome-based study. *Schizophr Bull*. 2020;46(3):699–712.
16. Xia M, Womer FY, Chang M, et al. Shared and distinct functional architectures of brain networks across psychiatric disorders. *Schizophr Bull*. 2019;45(2):450–463.
17. Chao-Gan Y, Yu-Feng Z. DPARSF: A MATLAB toolbox for “pipeline” data analysis of resting-state fMRI. *Front Syst Neurosci*. 2010;4:13.
18. Yang GJ, Murray JD, Repovs G, et al. Altered global brain signal in schizophrenia. *Proc Natl Acad Sci U S A*. 2014;111(20):7438–7443.
19. Power JD, Mitra A, Laumann TO, Snyder AZ, Schlaggar BL, Petersen SE. Methods to detect, characterize, and remove motion artifact in resting state fMRI. *Neuroimage*. 2014;84:320–341.
20. Rousseeuw PJ. Silhouettes: A graphical aid to the interpretation and validation of cluster analysis. *J Comput Appl Math*. 1987;20:53–65.
21. Hirschfeld RM. Differential diagnosis of bipolar disorder and major depressive disorder. *J Affect Disord*. 2014;169(Suppl 1):S12–S16.
22. Terachi S, Yamada T, Pu S, Yokoyama K, Matsumura H, Kaneko K. Comparison of neurocognitive function in major depressive disorder, bipolar disorder, and schizophrenia in later life: a cross-sectional study of euthymic or remitted, non-demented patients using the Japanese version of the Brief Assessment of Cognition in Schizophrenia (BACS-J). *Psychiatry Res*. 2017;254:205–210.
23. Wei Y, Chang M, Womer FY, et al. Local functional connectivity alterations in schizophrenia, bipolar disorder, and major depressive disorder. *J Affect Disord*. 2018;236:266–273.
24. Yang Y, Liu S, Jiang X, et al. Common and specific functional activity features in schizophrenia, major depressive disorder, and bipolar disorder. *Front Psychiatry*. 2019;10:52.
25. Tu PC, Bai YM, Li CT, et al. Identification of common thalamocortical dysconnectivity in four major psychiatric disorders. *Schizophr Bull*. 2019;45(5):1143–1151.
26. Brandl F, Avram M, Weise B, et al. Specific substantial dysconnectivity in schizophrenia: a transdiagnostic multimodal meta-analysis of resting-state functional and structural magnetic resonance imaging studies. *Biol Psychiatry*. 2019;85(7):573–583.
27. Sharma A, Wolf DH, Ciric R, et al. Common dimensional reward deficits across mood and psychotic disorders: a connectome-wide association study. *Am J Psychiatry*. 2017;174(7):657–666.
28. Baynes D, Mulholland C, Cooper SJ, et al. Depressive symptoms in stable chronic schizophrenia: prevalence and relationship to psychopathology and treatment. *Schizophr Res*. 2000;45(1-2):47–56.
29. Bjorkquist OA, Olsen EK, Nelson BD, Herbener ES. Altered amygdala-prefrontal connectivity during emotion perception in schizophrenia. *Schizophr Res*. 2016;175(1-3):35–41.
30. Mukherjee P, Whalley HC, McKirdy JW, et al. Altered amygdala connectivity within the social brain in schizophrenia. *Schizophr Bull*. 2014;40(1):152–160.
31. Sheffield JM, Barch DM. Cognition and resting-state functional connectivity in schizophrenia. *Neurosci Biobehav Rev*. 2016;61:108–120.
32. Kaufmann T, Skåtun KC, Alnæs D, et al. Disintegration of sensorimotor brain networks in schizophrenia. *Schizophr Bull*. 2015;41(6):1326–1335.
33. Wang X, Xia M, Lai Y, et al. Disrupted resting-state functional connectivity in minimally treated chronic schizophrenia. *Schizophr Res*. 2014;156(2-3):150–156.
34. Shinn AK, Baker JT, Cohen BM, Ongür D. Functional connectivity of left Heschl's gyrus in vulnerability to auditory hallucinations in schizophrenia. *Schizophr Res*. 2013;143(2-3):260–268.
35. Javitt DC, Freedman R. Sensory processing dysfunction in the personal experience and neuronal machinery of schizophrenia. *Am J Psychiatry*. 2015;172(1):17–31.
36. Guo W, Xiao C, Liu G, et al. Decreased resting-state interhemispheric coordination in first-episode, drug-naive paranoid schizophrenia. *Prog Neuropsychopharmacol Biol Psychiatry*. 2014;48:14–19.
37. Lui S, Li T, Deng W, et al. Short-term effects of antipsychotic treatment on cerebral function in drug-naive first-episode schizophrenia revealed by “resting state”

- functional magnetic resonance imaging. *Arch Gen Psychiatry*. 2010;67(8):783–792.
38. Pettersson-Yeo W, Allen P, Benetti S, McGuire P, Mechelli A. Dysconnectivity in schizophrenia: where are we now? *Neurosci Biobehav Rev*. 2011;35(5):1110–1124.
 39. Wang G, Lyu H, Wu R, Ou J, Zhu F, Liu Y, Zhao J, Guo W. Resting-state functional hypoconnectivity of amygdala in clinical high risk state and first-episode schizophrenia. *Brain Imaging Behav* 2019. doi:10.1007/s11682-019-00124-5.
 40. Tregellas JR, Davalos DB, Rojas DC, et al. Increased hemodynamic response in the hippocampus, thalamus and prefrontal cortex during abnormal sensory gating in schizophrenia. *Schizophr Res*. 2007;92(1-3):262–272.
 41. Danos P, Guich S, Abel L, Buchsbaum MS. Eeg alpha rhythm and glucose metabolic rate in the thalamus in schizophrenia. *Neuropsychobiology*. 2001;43(4):265–272.
 42. Merritt K, Egerton A, Kempton MJ, Taylor MJ, McGuire PK. Nature of glutamate alterations in schizophrenia: a meta-analysis of proton magnetic resonance spectroscopy studies. *JAMA Psychiatry*. 2016;73(7):665–674.
 43. Bartolomeo LA, Wright AM, Ma RE, et al. Relationship of auditory electrophysiological responses to magnetic resonance spectroscopy metabolites in Early Phase Psychosis. *Int J Psychophysiol*. 2019;145:15–22.
 44. Hanlon FM, Shaff NA, Dodd AB, et al. Hemodynamic response function abnormalities in schizophrenia during a multisensory detection task. *Hum Brain Mapp*. 2016;37(2):745–755.
 45. Alnæs D, Kaufmann T, van der Meer D, et al.; Karolinska Schizophrenia Project Consortium. Brain heterogeneity in schizophrenia and its association with polygenic risk. *JAMA Psychiatry*. 2019;76(7):739–748.
 46. Brugger SP, Howes OD. Heterogeneity and homogeneity of regional brain structure in schizophrenia: a meta-analysis. *JAMA Psychiatry*. 2017;74(11):1104–1111.
 47. Nenadic I, Gaser C, Sauer H. Heterogeneity of brain structural variation and the structural imaging endophenotypes in schizophrenia. *Neuropsychobiology*. 2012;66(1):44–49.
 48. Wolfers T, Doan NT, Kaufmann T, et al. Mapping the heterogeneous phenotype of schizophrenia and bipolar disorder using normative models. *JAMA Psychiatry*. 2018;75(11):1146–1155.
 49. Suárez LE, Markello RD, Betzel RF, Misic B. Linking structure and function in macroscale brain networks. *Trends Cogn Sci*. 2020;24(4):302–315.
 50. Vercammen A, Knegtering H, den Boer JA, Liemburg EJ, Aleman A. Auditory hallucinations in schizophrenia are associated with reduced functional connectivity of the temporo-parietal area. *Biol Psychiatry*. 2010;67(10):912–918.
 51. Eddy CM. The junction between self and other? Temporo-parietal dysfunction in neuropsychiatry. *Neuropsychologia*. 2016;89:465–477.
 52. McKay CM, Headlam DM, Copolov DL. Central auditory processing in patients with auditory hallucinations. *Am J Psychiatry*. 2000;157(5):759–766.
 53. Sedman G. Theories of depersonalization: a re-appraisal. *Br J Psychiatry*. 1970;117(536):1–14.
 54. Ionta S, Gassert R, Blanke O. Multi-sensory and sensorimotor foundation of bodily self-consciousness - an interdisciplinary approach. *Front Psychol*. 2011;2:383.
 55. Ionta S, Heydrich L, Lenggenhager B, et al. Multisensory mechanisms in temporo-parietal cortex support self-location and first-person perspective. *Neuron*. 2011;70(2):363–374.
 56. Waltz JA, Frank MJ, Robinson BM, Gold JM. Selective reinforcement learning deficits in schizophrenia support predictions from computational models of striatal-cortical dysfunction. *Biol Psychiatry*. 2007;62(7):756–764.
 57. Strauss GP, Frank MJ, Waltz JA, Kasanova Z, Herbener ES, Gold JM. Deficits in positive reinforcement learning and uncertainty-driven exploration are associated with distinct aspects of negative symptoms in schizophrenia. *Biol Psychiatry*. 2011;69(5):424–431.
 58. Das P, Kemp AH, Liddell BJ, et al. Pathways for fear perception: modulation of amygdala activity by thalamo-cortical systems. *Neuroimage*. 2005;26(1):141–148.
 59. Cao H, Bertolino A, Walter H, et al. Altered functional sub-network during emotional face processing: a potential intermediate phenotype for schizophrenia. *JAMA Psychiatry*. 2016;73(6):598–605.
 60. Eom TY, Bayazitov IT, Anderson K, Yu J, Zakharenko SS. Schizophrenia-Related microdeletion impairs emotional memory through microRNA-dependent disruption of thalamic inputs to the amygdala. *Cell Rep*. 2017;19(8):1532–1544.
 61. Honey GD, Pomarol-Clotet E, Corlett PR, et al. Functional dysconnectivity in schizophrenia associated with attentional modulation of motor function. *Brain*. 2005;128(Pt 11):2597–2611.
 62. Bracht T, Schnell S, Federspiel A, et al. Altered cortico-basal ganglia motor pathways reflect reduced volitional motor activity in schizophrenia. *Schizophr Res*. 2013;143(2-3):269–276.
 63. Martino M, Magioncalda P, Yu H, et al. Abnormal resting-state connectivity in a substantia nigra-related striato-thalamo-cortical network in a large sample of first-episode drug-naïve patients with schizophrenia. *Schizophr Bull*. 2018;44(2):419–431.
 64. Northoff G, Hirjak D, Wolf RC, Magioncalda P, Martino M. All roads lead to the motor cortex: psychomotor mechanisms and their biochemical modulation in psychiatric disorders. *Mol Psychiatry*. 2020. doi: 10.1038/s41380-020-0814-5.
 65. Snyder SH. The dopamine hypothesis of schizophrenia: focus on the dopamine receptor. *Am J Psychiatry*. 1976;133(2):197–202.
 66. Howes OD, Kapur S. The dopamine hypothesis of schizophrenia: version III—the final common pathway. *Schizophr Bull*. 2009;35(3):549–562.
 67. Brown RG, Pluck G. Negative symptoms: the ‘pathology’ of motivation and goal-directed behaviour. *Trends Neurosci*. 2000;23(9):412–417.
 68. Pralong E. Cellular perspectives on the glutamate–monoamine interactions in limbic lobe structures and their relevance for some psychiatric disorders. *Prog Neurobiol*. 2002;67(3):173–202.
 69. Giraldo-Chica M, Woodward ND. Review of thalamocortical resting-state fMRI studies in schizophrenia. *Schizophr Res*. 2017;180:58–63.
 70. Pergola G, Selvaggi P, Trizio S, Bertolino A, Blasi G. The role of the thalamus in schizophrenia from a neuroimaging perspective. *Neurosci Biobehav Rev*. 2015;54:57–75.
 71. Hua J, Blair NIS, Paez A, et al. Altered functional connectivity between sub-regions in the thalamus and cortex in schizophrenia patients measured by resting state BOLD fMRI at 7T. *Schizophr Res*. 2019;206:370–377.
 72. Cheng W, Palaniyappan L, Li M, et al. Voxel-based, brain-wide association study of aberrant functional connectivity in schizophrenia implicates thalamocortical circuitry. *npj Schizophr*. 2015;1:15016.

73. Jiang L, Xu Y, Zhu XT, Yang Z, Li HJ, Zuo XN. Local-to-remote cortical connectivity in early- and adulthood-onset schizophrenia. *Transl Psychiatry*. 2015;5:e566.
74. Li HJ, Xu Y, Zhang KR, Hoptman MJ, Zuo XN. Homotopic connectivity in drug-naïve, first-episode, early-onset schizophrenia. *J Child Psychol Psychiatry*. 2015;56(4):432–443.
75. Zheng J, Zhang Y, Guo X, Duan X, Zhang J, Zhao J, Chen H. Disrupted amplitude of low-frequency fluctuations in antipsychotic-naïve adolescents with early-onset schizophrenia. *Psychiatry Res Neuroimaging* 2016;249:20–26.
76. Kaufmann T, Alnæs D, Doan NT, Brandt CL, Andreassen OA, Westlye LT. Delayed stabilization and individualization in connectome development are related to psychiatric disorders. *Nat Neurosci*. 2017;20(4):513–515.
77. Zhang Y, Xu L, Hu Y, Wu J, Li C, Wang J, Yang Z. Functional connectivity between sensory-motor subnetworks reflects the duration of untreated psychosis and predicts treatment outcome of first-episode drug-naïve schizophrenia. *Biological Psychiatry: Cognitive Neuroscience and Neuroimaging* 2019;4(8):697–705.
78. Kraguljac NV, White DM, Hadley JA, et al. Abnormalities in large scale functional networks in unmedicated patients with schizophrenia and effects of risperidone. *Neuroimage Clin*. 2016;10:146–158.
79. Lee H, Lee DK, Park K, Kim CE, Ryu S. Default mode network connectivity is associated with long-term clinical outcome in patients with schizophrenia. *Neuroimage Clin*. 2019;22:101805.
80. Zhang L, Wang H, Luan S, et al. Altered volume and functional connectivity of the habenula in schizophrenia. *Front Hum Neurosci*. 2017;11:636.
81. Yao L, Li F, Liu J, et al. Functional brain networks in never-treated and treated long-term ill schizophrenia patients. *Neuropsychopharmacology*. 2019;44(11):1940–1947.
82. Kraguljac NV, White DM, Hadley N, et al. Aberrant hippocampal connectivity in unmedicated patients with schizophrenia and effects of antipsychotic medication: a longitudinal resting state functional MRI Study. *Schizophr Bull*. 2016;42(4):1046–1055.
83. Zong X, Hu M, Pantazatos SP, et al. A Dissociation in effects of risperidone monotherapy on functional and anatomical connectivity within the default mode network. *Schizophr Bull*. 2019;45(6):1309–1318.
84. Dawson N, Morris BJ, Pratt JA. Subanaesthetic ketamine treatment alters prefrontal cortex connectivity with thalamus and ascending subcortical systems. *Schizophr Bull*. 2013;39(2):366–377.
85. Li H, Ou Y, Liu F, et al. Reduced connectivity in anterior cingulate cortex as an early predictor for treatment response in drug-naïve, first-episode schizophrenia: a global-brain functional connectivity analysis. *Schizophr Res*. 2020;215:337–343.
86. Finn ES, Todd Constable R. Individual variation in functional brain connectivity: implications for personalized approaches to psychiatric disease. *Dialogues Clin Neurosci*. 2016;18(3):277–287.
87. Drysdale AT, Grosenick L, Downar J, et al. Resting-state connectivity biomarkers define neurophysiological subtypes of depression. *Nat Med*. 2017;23(1):28–38.
88. Fox MD, Liu H, Pascual-Leone A. Identification of reproducible individualized targets for treatment of depression with TMS based on intrinsic connectivity. *Neuroimage*. 2013;66:151–160.
89. Chang M, Womer FY, Edmiston EK, et al. Neurobiological commonalities and distinctions among three major psychiatric diagnostic categories: a structural MRI Study. *Schizophr Bull*. 2018;44(1):65–74.
90. Sha Z, Wager TD, Mechelli A, He Y. Common dysfunction of large-scale neurocognitive networks across psychiatric disorders. *Biol Psychiatry*. 2019;85(5):379–388.
91. Birn RM, Molloy EK, Patriat R, et al. The effect of scan length on the reliability of resting-state fMRI connectivity estimates. *Neuroimage*. 2013;83:550–558.
92. Noble S, Spann MN, Tokoglu F, Shen X, Constable RT, Scheinost D. Influences on the test-retest reliability of functional connectivity MRI and its relationship with behavioral utility. *Cereb Cortex*. 2017;27(11):5415–5429.